Applied Thermal Engineering 104 (2016) 734–742

Contents lists available at ScienceDirect

Applied Thermal Engineering

journal homepage: www.elsevier.com/locate/apthermeng

Research Paper

# A continuous desalination system using humidification – dehumidification and a solar still with an evacuated solar water heater

S.W. Sharshir [a,b,c], Guilong Peng [a,b], Nuo Yang [a,b,*], M.O.A. El-Samadony [c], A.E. Kabeel [d]

[a] Nano Interface Center for Energy (NICE), School of Energy and Power Engineering, Huazhong University of Science and Technology, Wuhan 430074, PR China
[b] State Key Laboratory of Coal Combustion, Huazhong University of Science and Technology, Wuhan 430074, PR China
[c] Mechanical Engineering Department, Faculty of Engineering, Kafrelsheikh University, Kafrelsheikh, Egypt
[d] Mechanical Power Engineering Department, Faculty of Engineering, Tanta University, Tanta, Egypt

## HIGHLIGHTS

- The different water mass flow rate on HDH is investigated.
- Enhancement of the gain output ratio of the desalination unit.
- Enhancing the thermal performance of the desalination unit with reusing rejected water from HDH.

## ARTICLE INFO

*Article history:*
Received 1 September 2015
Revised 16 May 2016
Accepted 20 May 2016
Available online 21 May 2016

*Keywords:*
Humidification–dehumidification
Solar still
Solar desalination
Energy balance
Mass balance
GOR

## ABSTRACT

A continuous solar still (SS) integrated with a solar humidification–dehumidification (HDH) is investigated. An evacuated solar water collector is utilized in the HDH. The idea of closed-air and open-water cycles is considered as the operating principle of HDH process. The different water mass flow rates (1.5, 2, 2.5 and 3 L/min) of HDH is investigated. To avoid a large water loss during HDH desalination, a SS is fed with the exit warm water from HDH during day and night time. Therefore, the productivity of the SS with exit warm water from HDH is greater than that of the conventional solar still (CSS) by approximately 242% and the gain output ratio (GOR) is increased by about 39%. The daily water productions of the CSS, SS with exit warm water from HDH, HDH unit and continuous solar desalination unit are 3.9, 13, 24 and 37 L/day, respectively.



## 1. Introduction

Everything in the world, either for society or personal using, needs water. Unfortunately, only less than 0.1% of the existing water covering 71% of the earth's surface is accessible potable water [1]. Improving the effectiveness and efficiency of water purification technology is considered by many as perhaps the main challenge of the 21st century [2]. Therefore, intensive efforts are underway throughout the world to avert this looming crisis with conservation of the existing limited freshwater supply and conversion of the abundantly available seawater through various desalting technologies.

Humidification–dehumidification (HDH) desalination is a simple technology that is similar to rain cycle and has the possibility to carry out with solar heating [3,4]. The various system configurations of HDH, operating and meteorological conditions of a solar distillation system have been investigated in details [5,6]

Hamed et al. [7] investigated mathematically and experimentally a solar HDH system. They got high productivity of about 22 L/day due to preheating. The exergy analysis of HDH unit has been afforded [8]. The collector has lowest exergy efficiency and HDH process has lower exergy efficiency but the exit warm water from HDH has great exergy loss. Many improvements can be made on HDH process. Three ways were proposed to enhance freshwater yield per square meter area of collector. The first way depends on increasing both exergy and energy efficiencies and that is, to take measures for extra amount of energy and extra exergy. The second way is to enhance the flow of HDH process in order to gain a high-energy recover rate and the gain output ratio (GOR). Finally, the third way is based on reusing the exit warm water to get freshwater.

Zhani [9] has used the solar energy to generate a desalinate water depending on the HDH principle. Yıldırım and Solmuş [10]

* Corresponding author.
*E-mail address:* nuo@hust.edu.cn (N. Yang).

http://dx.doi.org/10.1016/j.applthermaleng.2016.05.120
1359-4311/

**Nomenclature**

| | |
|---|---|
| $a$ | specific area of evaporator, $m^2/m^3$ |
| $A$ | area of SS, $m^2$ |
| $A_C$ | external area of condenser surface, $m^2$ |
| $A_{cond}$ | evaporator area of heat transfer, $m^2$ |
| $A_E$ | external area of evaporator, $m^2$ |
| $Cp$ | heat capacity, J/kg °C |
| $Cp_a$ | heat capacity of air, 1.009 kJ/kg °C |
| $Cp_v$ | heat capacity of vapor, 1.88 kJ/kg °C |
| $Cp_w$ | heat capacity of liquid water, 4.193 kJ/kg °C |
| $Cp_b$ | heat capacity of liquid water brine assume = 4.193 kJ/kg °C |
| $e$ | correction factor for cross-flow heat and mass transfer |
| $H_a$ | enthalpy of saturated air, kJ/kg |
| $H_{aci}$ | condenser inlet air enthalpy, kJ/kg |
| $H_{ace}$ | condenser exit air enthalpy kJ/kg |
| $H_{ahi}$ | humidifier inlet air enthalpy, kJ/kg |
| $H_{ahe}$ | humidifier exit air enthalpy, kJ/kg |
| $h_{fg}$ | evaporation and condensation latent heat of, kJ/kg |
| $h_{bw}$ | convection heat transfer coefficient between the basin and water, W/$m^2$ °C |
| $h_{ca}$ | convection heat transfer coefficient with the ambient, W/$m^2$ °C |
| $h_{cw}$ | convection heat transfer coefficient between the water and glazier, W/$m^2$ °C |
| $h_{fgss}$ | latent heat of vaporization for SS, J/kg |
| $I(t)$ | solar insolation normal to glazier s cover, W/$m^2$ |
| $m$ | mass, L |
| $m_a$ | air mass flow rate, kg/s |
| $m_d$ | rate of desalinated water for HDH, kg/h |
| $mw$ | water flow rate, kg/min |
| $m_{re}$ | rejected water from HDH, L |
| $m_{dss}$ | rate of mass evaporation, L/s |
| $P_{am}$ | atmospheric pressure, kPa |
| $P_g$ | water vapor pressure at glass temperature, Pa |
| $P_w$ | water vapor pressure at water temperature, Pa |
| $P_{db}$ | water vapor pressure at the dry bulb temperature, kPa |
| $P_{st}$ | saturation pressure, kPa |
| $T_{ace}$ | air temperature at condenser exit, °C |
| $T_{aci}$ | air temperature at condenser inlet, °C |
| $T_{amb}$ | ambient temperature, °C |
| $T_{avgC}$ | average temperature in the condenser, °C |
| $T_{avgE}$ | average temperature in the, evaporator, °C |
| $T_{wce}$ | water temperature at condenser exit, °C |
| $T_{whe}$ | water temperature at humidifier exit, °C |
| $T_{whi}$ | water temperature at humidifier inlet, °C |
| $U$ | heat loss coefficient from basin and sides to ambient, W/$m^2$ K |
| $U_{cond}$ | over coefficient of heat transfer at condenser, J/$m^2$ s °C |
| $U_{LC}$ | over all heat loss coefficient for condenser, J/$m^2$ s °C |
| $U_{LE}$ | over all heat loss coefficient of evaporator, J/$m^2$ s °C |
| $V$ | evaporator volume, $m^3$ |
| $V_a$ | wind velocity, m/s |
| $W_{ace}$ | humidity ratio at condenser exit, $kg_v/kg_a$ |
| $W_{aci}$ | humidity ratio at condenser inlet, $kg_v/kg_a$ |
| $W_{ahe}$ | humidity ratio at humidifier exit, $kg_v/kg_a$ |
| $W_{ahi}$ | humidity ratio at humidifier inlet, $kg_v/kg_a$ |
| $W_{ast}$ | humidity ratio at saturation, $kg_v/kg_a$ |
| $Q_{bw}$ | heat transfer from basin to water in basin, W |
| $Q_{cg}$ | heat transfer from glass to ambient, W |
| $Q_{cw}$ | heat transfer from water in basin to glass, W |
| $Q_e$ | heat transfer due to evaporation, W |
| $Q_{loss}$ | heat transfer from basin to ambient, W |
| $Q_{mw}$ | energy needed to heat makeup water to water basin temperature, W |
| $Q_{rg}$ | radiation heat transfers from glass to ambient, W |
| $Q_{rw}$ | radiation heat transfers from water in basin to glazier, W |
| $T$ | temperature, °C |

*Greek letters*

| | |
|---|---|
| $\alpha$ | absorption coefficient |
| $\varepsilon$ | emissivity coefficient |
| $\sigma$ | Stefan–Boltzmann constant, W/$m^2$ $K^4$ |

*Subscripts*

| | |
|---|---|
| $a$ | air |
| $b$ | basin |
| $g$ | glass |
| $sky$ | sky |
| $w$ | basin water |

examined theoretically the performance of a solar HDH unit with different configurations such as water heating only, air heating only and water–air heating. Hou and Zhang [11] studied the hybrid multi effect HDH and the conventional type. The GOR was improved by 2–3.

The amount of condensed water in SS depends on the glass–water temperature difference. Increasing this difference increases the circulation of air inside the SS which is the main reason to increase the productivity in desalination process. Regenerative SS [12], double glasses [13] and triple-basin SS [14] were investigated. Preheating is a method for increasing the SS yield. The collector increases the thermal energy given to the saline water of the SS [15–17]

Yadav [18] evaluated the performance of a SS connected with a collector using the forced circulation and thermosyphon modes. In case of forced circulation style, the system gave approximately 5–10% greater production than that of thermosyphon mode whereas; 30–35% improvement was obtained with simple SS. The water depth strongly influences the SS productivity [19–22].

The principal components of the SS system were also presented and compared. According to energy analysis, using continuous solar desalination process aims at enhancement the freshwater output per square meter area of solar collector. Evacuated tube solar collector is involved in the desalination system to heat entering water to the humidifier and the exit warm water from HDH process is reused to feed SS during the day and night time.

The objective of this work is to improve the performance of HDH and SS by using exit warm water from HDH. The operation involves two steps. In the first theoretical and experimental step, HDH system operates from 13 pm to 18 pm and the exit warm water from the humidifier bottom with high temperature of about 66–75 °C moves to an insulated tank. In the second (theoretical) step, the stored water in the insulated tank feeds the single stage SS at high temperature (assumed $T_w$ = 70 °C). The exit warm water from HDH is of high temperature enough to feed water to SS during 24 h (change all water in the still basin every hour by warm water).

The contributions of this work are:

1. Increasing the output of the continuous system compared to HDH and CSS separately by using the exit warm water from HDH to feed CSS.
2. Increasing the thermal performance of the continuous system compared to HDH and CSS separately.

3. The different of feed water mass flow rates (1.5, 2, 2.5 and 3 L/min) on HDH performance was investigated.
4. SS with exit warm water from HDH can work during day and night time.

## 2. System description

Detailed drawing of the desalination unite is shown in Fig. 1. The solar HDH unit consists of two vertical ducts joined together from the top and the bottom making a closed loop for air circulation and open loop for water circulation. In a forced draft mode, the unit is run out by using a fan fixed at the bottom of the connection duct as illustrated in Kabeel et al. [23] A large surface condenser is settled in one of the two ducts (dehumidifier); whereas cellulose paper with opening packing of 5 mm and total surface area of approximately 10 $m^2$ is utilized in the other duct for more efficient humidification of the air (humidifier). Firstly, a cold-water pump is used to force the cold brackish water to move from the cold-water tank to enter the condenser. This cold water is used to condense partially the warm saturated air. The unsaturated cold air exits from the condenser (dehumidifier) bottom to enter the evaporator (humidifier) to become warm and saturated. The air is continuously heated and humidified (closed loop). The condensation latent heat is used to raise the temperature of the feed water. The preheated water leaves the condenser from the top to be further heated in an evacuated collector. By using a warm water pump, the warm water from the collector is forced to move to the humidifier inlet. Last, the feed water at humidifier inlet (at the top of humidifier) is sprayed through water sprayers over the cellulose packing in the humidifier. The exit warm water from the bottom of humidifier is pumped to an isolated tank to feed the SS then, the SS has a new advantage of working during daytime as well as nighttime. The description of the HDH unit is tabulated in Table 1.

## 3. Experimental procedures and error analysis for HDH system

The experiments were run out in the period from May to June 2014 at the Engineering Faculty, Kafrelsheikh University, Egypt (Latitude 31.07°N and longitude 30.57°E). The present experimental results illustrate that highest solar intensity is about 1050 W/$m^2$ at noon as shown in Fig 2. Stored energy in the collector from the morning to 13 pm increases its water temperature up to 85 °C.

Through the experiments, some parameters were gauged to obtain the system performance. The measured parameters are flow rates of water and air, inlet and exit water temperature from the tanks, temperatures of air and water at the inlet and exit of each tower, relative humidity of each tower and the yield of the unit. Table 2 illustrates the accuracy, range and uncertainty errors of each measuring instrument.

## 4. System process model

### 4.1. Energy and mass balance equations in HDH

To estimate the performance of HDH unit theoretically, a mathematical model is proposed through solving of the energy balance equations for collector, dehumidifier and humidifier. The air temperatures, water temperatures and productivity can be evaluated at various conditions are written here as in [7,24]

Assuming steady state condition, the energy balance in the dehumidifier element

$$m_a(H_{aci} - H_{ace}) + m_{fw}Cp_w(T_{wci} - T_{wce}) - U_{LC}A_C(T_{avgC} - T_{amb}) = 0 \quad (1)$$

The total heat transfer rate in condenser as a faction in LMTD

$$mwCp_w(T_{wce} - T_{wci}) = eU_{cond}A_{cond}\left[\frac{(T_{aci} - T_{wce}) - (T_{ace} - T_{wci})}{\ln\frac{(T_{aci} - T_{wce})}{(T_{ace} - T_{wci})}}\right] \quad (2)$$

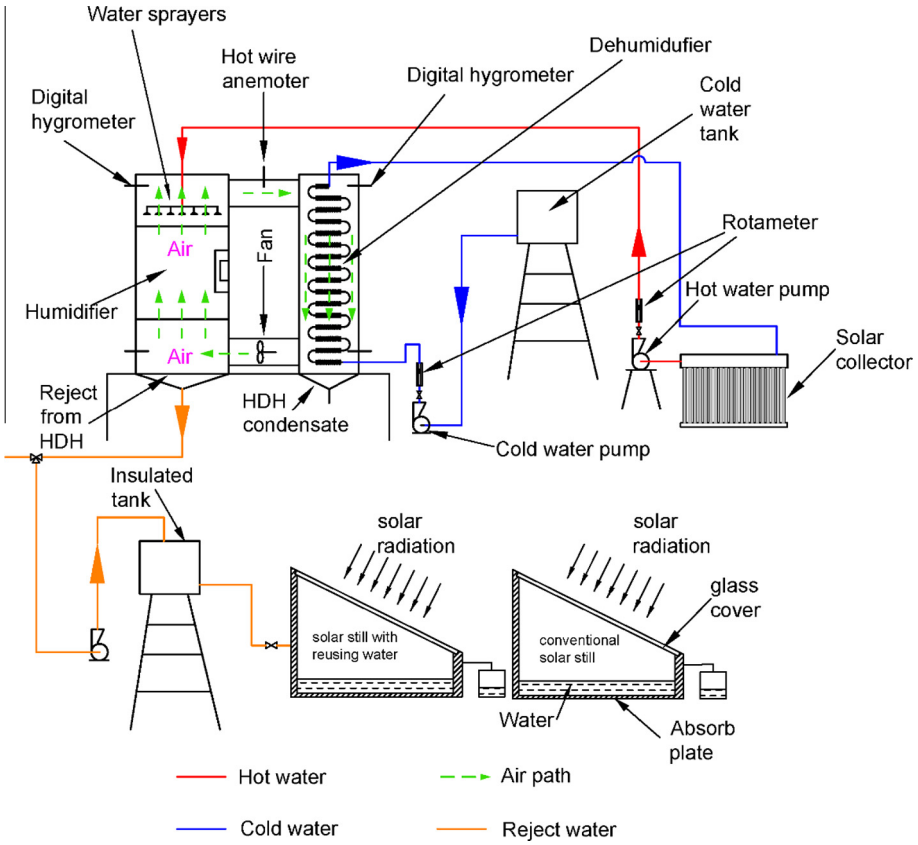


**Fig. 1.** Schematic diagram of the experimental setup.

**Table 1**
System technical specifications data used for Hybrid HDH–SS.

| Technical specification | Value |
|---|---|
| *Humidifier* | |
| Galvanized steel thickness, mm | 1.5 |
| Rectangular cross sectional area, cm | 50 × 80 |
| Height, cm | 200 |
| Packing material, honey comb shape with total surface area, $m^2$ | 10 |
| *Dehumidifier* | |
| Galvanized steel thickness, mm | 1.5 |
| Cylindrical shape with diameter, cm | 40 |
| Height, cm | 200 |
| Coil which is a copper tube of length, m | 15 |
| Thickness of coil, mm | 1.5 |
| Outer diameter, cm | 1.27 |
| *Mounted by copper corrugated fins* | |
| Vacuum tube solar collector | |
| Total projected area, $m^2$ | 2 |
| Vacuum tubes | 20 |
| A cylindrical stainless steel water tank, insulated with polyurethane foam, Thickness, cm | 5 |
| Capacity, L | 220 |
| *Pumps and fans* | |
| Three centrifugal pumps power, W | 373 |
| One electric fan power, W | 15 |
| *Water storage tank* | |
| Cold water tank having a volume, L | 250 |
| Made from Polyvinyl Chloride (PVC) with thickness, mm | 2 |
| Insolated hot water tank having a volume, L | 220 |
| Made from steel with thickness, mm | 1.5 |
| *Solar stills* | |
| Basin area, $m^2$ | 1.16 |
| Basin dimension, m | 1 × 16 |
| High-side wall depth, m | 0.450 |
| Low side wall depth, m | 0.160 |
| Glass cover with thickness, mm | 3 |

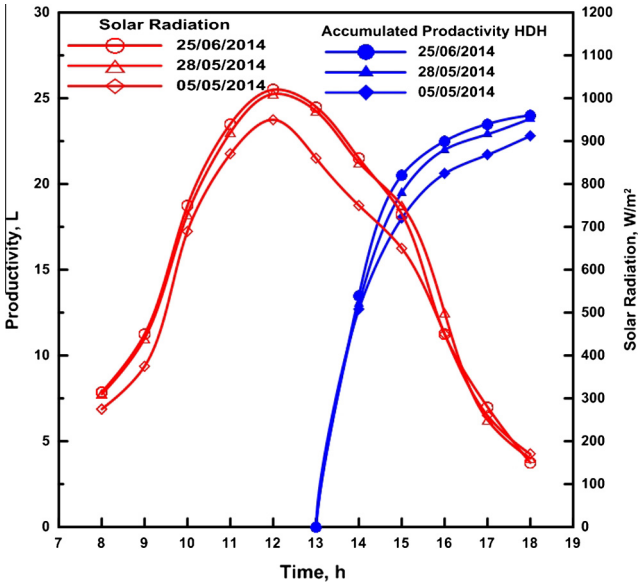


**Fig. 2.** Shows the accumulated productivity starting from 13:18 pm.

Assuming steady state condition, energy balance in the humidifier can be written as

$$m_a(H_{ahi} - H_{ahe}) + m_{fw}Cp_w(T_{whi} - T_{whe}) - U_{LE}A_E(T_{avgE} - T_{amb}) = 0 \quad (3)$$

The mass transfer rate in the humidifier as a faction in LMTD can be written as

**Table 2**
Experimental measurements, Accuracy, range, uncertainty errors.

| Instrument | Accuracy | Range | % Error |
|---|---|---|---|
| Solar meter, to measure solar radiation | ±1 W/$m^2$ | 0–2000 W/$m^2$ | 1.5 |
| Temperature indicator, thermocouples of K-type | ±0.1 °C | 0–100 °C | 1.5 |
| Humidity sensor, to measure the relative humidity | ±1.5% RH | 0–100% RH | 1 |
| Air flow meter, to measure air velocity | ±0.1 m/s | 0.0–10 m/s | 0.75 |
| Water flow meter, to measure either cold or hot water flow rate, liter per minute (LPM) | ±0.1 LPM | 0.02–8 LPM | 1 |

$$m_a(H_{ahe} - H_{ahi}) = ekaV_E\left[\frac{(H_{whi} - H_{ahe}) - (H_{whe} - H_{ahi})}{\ln\frac{(H_{whi} - H_{ahi})}{(H_{whe} - H_{ahi})}}\right] \quad (4)$$

where $e$ is the factor of correction for cross-flow heat transfer and it equals unity for condensation and boiling regardless the flow arrangement [7].

The energy balance in solar collector is written as in [7].

$$\dot{Q}_{solar} = m_{fw}Cp_w(T_{whi} - T_{wce}) \quad (5)$$

The distillate flow rate is obtained by the mass balance assuming the change of water content between the air entering and leaving the dehumidifier. This rate of purification is given as in [7,24],

$$m_{dHDH} = m_a(W_{aci} - W_{ace}) \quad (6)$$

The amount of water exit from humidifier can be calculated by:

$$m_{whe} = m_{fwHDH} - m_{dHDH} \quad (7)$$

$$m_{whe} = m_{fwHDH} - (W_{aci} - W_{ace})m_a \quad (8)$$

For solving the governing system of equations that illustrates the mathematical modeling for humidifier, dehumidifier and solar heater, the next parameters are considered to be known. Flow rates: $m_a$ and $m_{fw}$, Properties $Cp_w$, $Cp_a$, $Cp_b$, $Cp_v$, $H_{vap}$, $P_{atm}$, External geometry $A_C$, $A_E$, Internal geometry: $A_{cond}$, $a$, $V$, $(T_{ace} = T_{ahi},\ T_{aci} = T_{ahe})$, $T_{wci}$, $T_{amb}$, $T_{wce}$. These parameters are used to calculated the mean values of heat and mass transfer, $U_{LE}$, $U_{cond}$, $U_{LC}$ and $K$ coefficients using Matlab program which are 24.254, 23.254, 147.056 and 0.17 respectively.

### 4.2. Theoretical modeling for solar still

The energy balance for the SS should be presented for three regions: brackish water, absorber plate and glass cover. The temperatures of saline water, basin plate and glass cover can be estimated at every moment. By the use of Matlab program, the differential equation can be solved. The next assumptions are taken into consideration for the SS energy equations:

- Steady state conditions through the SSs.
- The glazier cover is suggested to be thin enough to render absorption of any incident radiation and the glazier conduction resistance could be neglected.
- The SSs prevent leakage of vapor.

Energy balance for the absorber plate [25]

$$m_b c_{pb}(dT_b/dt) = I(t)A_b\alpha_b - Q_{bw} - Q_{loss} \quad (9)$$

Energy balance for the brackish water [25,26],

$$m_w c_{pw}(dT_w/dt) = I(t)A_w\alpha_w + Q_{bw} - Q_{cw} - Q_{rw} - Q_e - Q_{mw} \quad (10)$$

Energy balance for the glazier cover [25]

$$m_g c_{pg}(dT_g/dt) = I(t)A_g\alpha_g + Q_{cw} + Q_{rw} + Q_e - Q_{rg} - Q_{cg} \quad (11)$$

The convective heat transfer rate between basin plate and brackish water [27,28],

$$Q_{bw} = h_{bw}A_b(T_b - T_w) \quad (12)$$

The convective heat transfer coefficient between basin plate and brackish water, $h_{bw}$ is assumed as 135 W/m$^2$ K [27,28].

The rate of heat losses by convection through the basin and sides to the ground and ambient is given as [29],

$$Q_{loss} = U_b A_b \times (T_b - T_a) \quad (13)$$

where $U_b$ is taken, 14 W/m$^2$ K as [26].

The convective heat transfer rate between water and glazier cover is given by [27,28],

$$Q_{cw} = h_{cw}A_w(T_w - T_g) \quad (14)$$

where the convective heat transfer coefficient between water and glazier cover is given by [12],

$$h_{cw} = 0.884\left\{(T_w - T_g) + \frac{[p_w - p_g][T_w + 273.15]}{[268900 - p_w]}\right\}^{1/3} \quad (15)$$

where

$$P_w = e^{\left(25.317 - \frac{5144}{Tw+273}\right)} \quad (16)$$

$$P_g = e^{\left(25.317 - \frac{5144}{Tg+273}\right)} \quad (17)$$

The radiation heat transfer rate from the basin to glazier cover is predicted from [26],

$$Q_{rw} = \sigma\varepsilon_{eq}A_w\left[(T_w + 273)^4 - (T_g + 273)^4\right] \quad (18)$$

where

$$\varepsilon_{eq} = \left[\frac{1}{\varepsilon_w} + \frac{1}{\varepsilon_g} - 1\right]^{-1} \quad (19)$$

The evaporative heat transfer rate between water and glazier is given by [27,28],

$$Q_e = (16.237\text{X}10^{-3})h_{cw}A_w(P_w - P_g) \quad (20)$$

It is also assumed that, the makeup water is at ambient temperature and takes heat from basin. The heat taken by the replaced water is estimated from [26],

$$Q_{mw} = m_{re}C_w(T_a - T_w) \quad (21)$$

The heat transfer rate by radiation between glazier cover and sky $Q_{rg}$ is given by [27,28],

$$Q_{rg} = \varepsilon_g A_g \sigma[(T_g + 273)^4 - (T_{sky} + 273)^4] \quad (22)$$

The sky temperature is taken from [12],

$$T_{sky} = T_a - 6.0 \quad (23)$$

The convective heat transfer rate between glazier cover and sky is given by [30],

$$Q_{cg} = h_{ca}A_g(T_g - T_{sky}) \quad (24)$$

where $h_{ac}$ is taken from [12],

$$h_{ca} = 2.80 + 3.0 \times V_a \quad (25)$$

SS productivity

$$m_{dss} = \frac{Q_e}{h_{fgss}} \quad (26)$$

At the first iteration, water and glazier temperature are taken as ambient temperature, but basin temperature is taken as 70 °C and the increase in basin plate temperature ($dT_b$), brackish water temperature ($dT_w$) and glass cover temperature ($dT_g$) are computed by solving Eqs. (9)–(11), for CSS. The equations are evaluated numerically using the first order backward difference formula. The size of the time step is 1 s. In the next time step, the parameters are redefined as follows $T_b = T_b + dT_b$, $T_w = T_w + dT_w$ and $T_g = T_g + dT_g$ (see appendix. for the program flow chart). To be very close to real ambient conditions, solar intensity $I(t)$ and surrounding temperature ($T_a$) are measured at different days from 8 am to 18 pm during the period from May to June 2014 at the Engineering Faculty, Kafrelsheikh University, Egypt. Depending upon the weather conditions, the wind speed is varied from 0.3 to 6.5 m/s and the ambient air temperature is varied from 22 to 34 °C at different days and solar intensity is varied from 35 to 1050 W/m$^2$. The physical and operating parameters used in the theoretical calculations are shown in Table 3. The physical parameters used are taken as that of Ref. [31].

## 5. System performance assessment

In order to properly asses the feasibility of the proposed system. Many parameters are often used for describing the performance of desalination systems. The gain output ratio. (GOR) it is defined as the ratio of the evaporation latent heat of the produced water to the net heat input to the unit. The thermal performance of HDH is defined as [7]:

$$GOR_{HDH} = \frac{\dot{m}_p h_{fg}}{Q_{in}} \quad (27)$$

The thermal performance gained by SS is define as.

$$GOR_{SS} = \frac{(m_{dsswithHDH} - m_{dconvitional})h_{fg}}{Q_{in}} \quad (28)$$

The performance of the (HDH–SS) desalinate unit is calculated as [11]:

$$\text{GOR}_{sys} = GOR_{HDH} + GOR_{SS} \quad (29)$$

## 6. Results and discussion

### 6.1. HDH daily productivity

The experimental results illustrate that highest solar intensity is about 1050 W/m$^2$ at noon as show in Fig. 2. Stored energy in the collector from the morning up to 13 pm raises the water temperature in the collector to reach 85 °C at 2.5 L/min. Fig. 2 shows the variation of the accumulated productivity and solar intensity with time during three different days. From the figure, the first hour (13:14 pm) of operation gives the highest productivity of nearly 13.5 L/h due to the higher temperature of water entering the evaporator from collector and then the productivity reduces until it reaches the lowest value of about 0.9 L at 17:18 pm owing to the lower temperature of the water entering the humidifier. The accumulated productivity reaches a value of approximately 24 L/day.

**Table 3**
Physical and operating parameters used in the theoretical calculation [31].

| Item | Mass (kg) | Area (m$^2$) | Specific heat (J/kg K) | Absorptivity | Emissivity |
|---|---|---|---|---|---|
| Saline water | 5.9 | 1.16 | 4190 | 0.05 | 0.96 |
| Glass cover | 9 | 1.12 | 840 | 0.05 | 0.85 |
| Basin plate | 14.5 | 1.16 | 460 | 0.95 | – |

Latent heat at $h_{fgss}$ = 2,335,000 J/kg.

The results of HDH are validated by comparing the results from the experimental data with the theoretical. The experimental system was started up relying on the collector and was neglected for a long time enough to reach steady state condition. Fig. 3 shows a comparison between the calculated and the measured productivity of the system. A good agreement is obtained from the validation between the experimental and theoretical data.

### 6.2. Effect of temperatures on HDH performance

The effects of variation of humidifier inlet water temperature ($T_{whi}$), humidifier exit water temperature ($T_{whe}$), condenser inlet air temperature ($T_{wci}$) and condenser exit air temperature ($T_{wce}$), with time are shown in Fig. 4. From the figure, all temperatures are affected by the humidifier inlet water temperature. At the first operation, all temperatures are high due to the high $T_{whi}$ then; they all decrease with time due to the decrease in the $T_{whi}$ so that the large productivity is obtained at the first hour of operation range from (66:75 °C) going to isolated tank and used to feed the SS during the daytime and nighttime.

### 6.3. Effect of water flow rate on the HDH performance

Fig. 5 shows a comparison between the cold and warm feed water at different flow rates. The various flow rates (1.5, 2, 2.5 and 3 L/min) affect the productivity. The figure shows that as the water flow rate increases, the productivity increases for the three tested cases (1.5, 2 and 2.5). In addition, any increase in the flow rate more than 2.5 will cause an increase at the first time of operation followed by a decrease in the productivity so that the best flow rate of warm and cold water equals to 2.5 L/min, this is because the vapor formation is better for the flow rates of (2.5 L/min). While for lower flow rates (1.5 and 2 L/min), the exit vapor from the sprayers looks like a free water stream. In contrast, the flow rate of 3 L/min exits from the sprayers as a jet. So, for the flow rates (1.5, 2 and 3 L/min), there is no chance to vaporize all of exit water from sprayers. On the second hand, most of the exit water from the sprayers are vaporized at 2.5 L/min.

Fig. 6 shows the difference between Ref. [7] and present work for HDH. In Ref. [7] Hamed et al. Studied the productivity at mw = 2 L/min but, in the present study, the productivity is at mw = 2.5 L/min. The figure illustrates that the first hour of operation (13:14 pm) gives the highest productivity of nearly 13.5 L/h due to the higher water temperature entering the humidifier from the collector and increasing the warm water mass flow rate at mw = 2.5 kg/min. Furthermore, the first hour of operation (13:14 pm) in the previous study gave the maximum productivity of nearly 11.2 L/h at mw = 2 L/min. In addition, in the present study, the time of operation is increased from 13 to 18 pm but in the previous study, it was from (15 to 17). In addition, the productivity of HDH in the present study is 24 L/day but it was 22 L/day in the previous work.

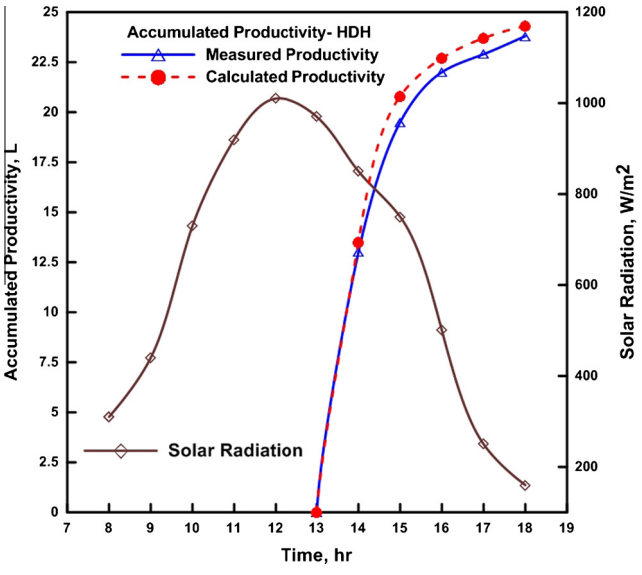


**Fig. 3.** Comparison between calculated and measured productivity of HDH.

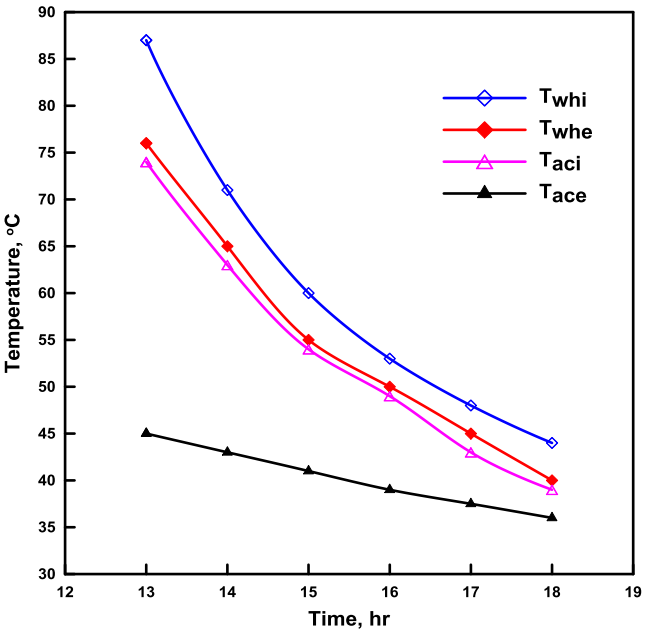


**Fig. 4.** The hourly temperature variation with time.

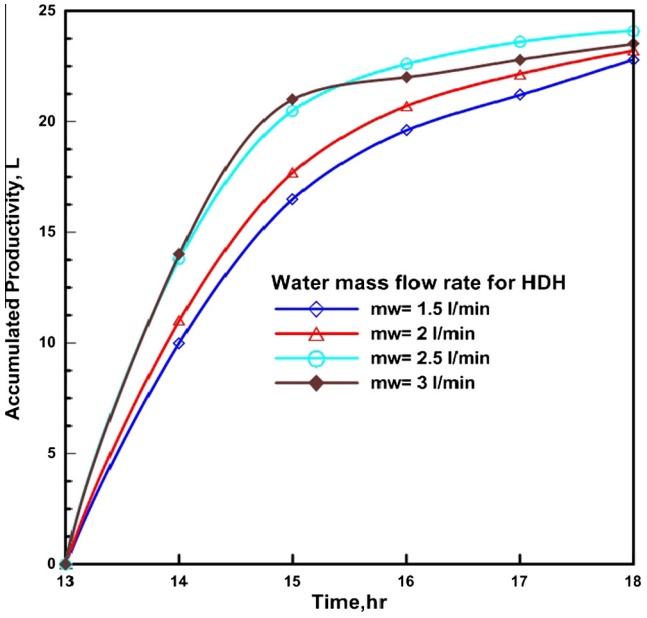


**Fig. 5.** Effect of feed water mass flow rate on the HDH performance.

### 6.4. Effect of solar intensity on solar still performance

Fig. 7 shows the variation of solar radiation, basin, water and glass temperature for CSS and SS with exit warm water from

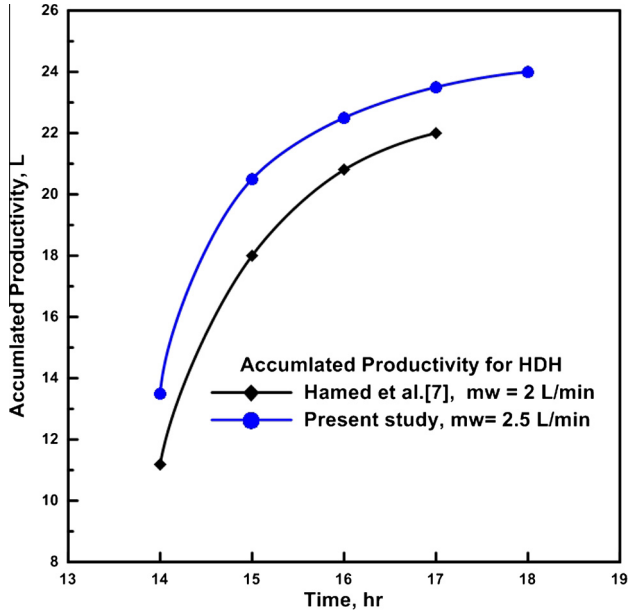


**Fig. 6.** Shows a difference between accumulated productivity of Ref. [7] and that of the present work.

HDH. The higher solar intensity, the higher SS performance. So the best performance is obtained at the period from 11 am up to 3 pm. Also, from figure, the basin, water and glass temperature of SS with exit warm water from HDH are higher than that of CSS by about 15–32 °C, 13–28 °C and 11–23 °C, respectively [due to using feed water from insulation tank with high temperature]. Using warm water gave better performance because warm water enhances energy input to the SS with exit warm water from HDH. The results indicated that, the basin plate glass temperature and basin water temperature of SS with HDH were higher than that of CSS type. Consequently, the evaporation and condensation rates in SS with exit warm water from HDH were increased.

### 6.5. Hourly water productivity for solar stills during the daytime

A theoretical comparison between the average hourly variation of freshwater productivity for SS with exit warm water from HDH

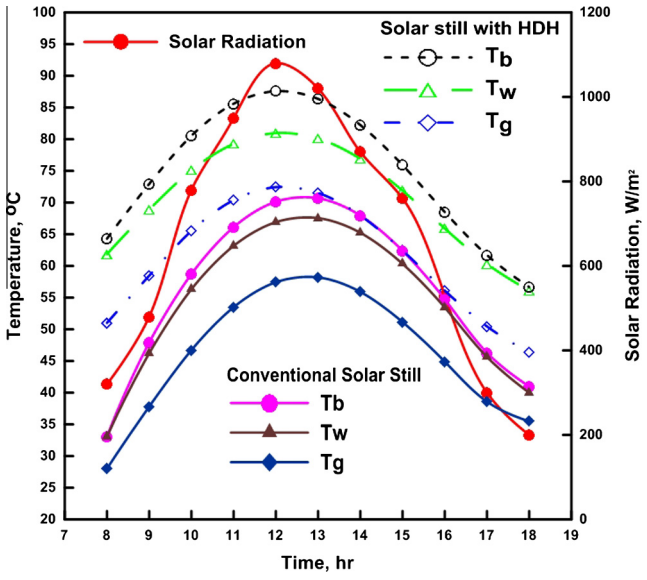


**Fig. 7.** The hourly temperature variation and solar radiation for SSs.

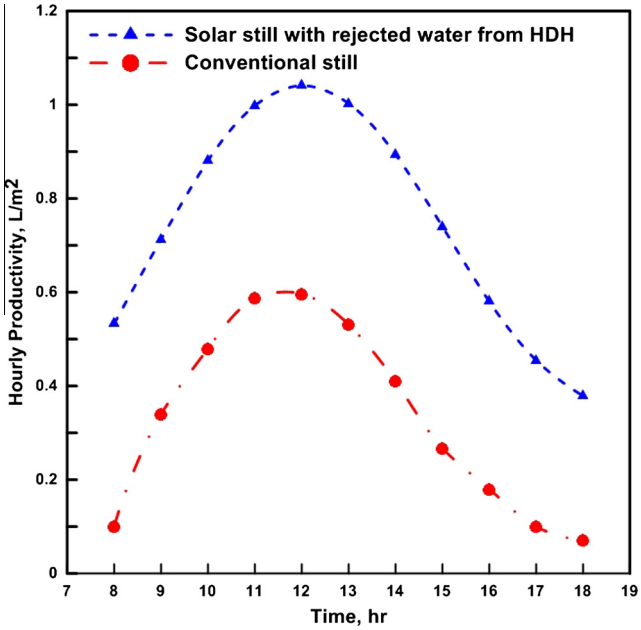


**Fig. 8.** Variation of freshwater productivity for the SS with HDH and the CSS during the daytime.

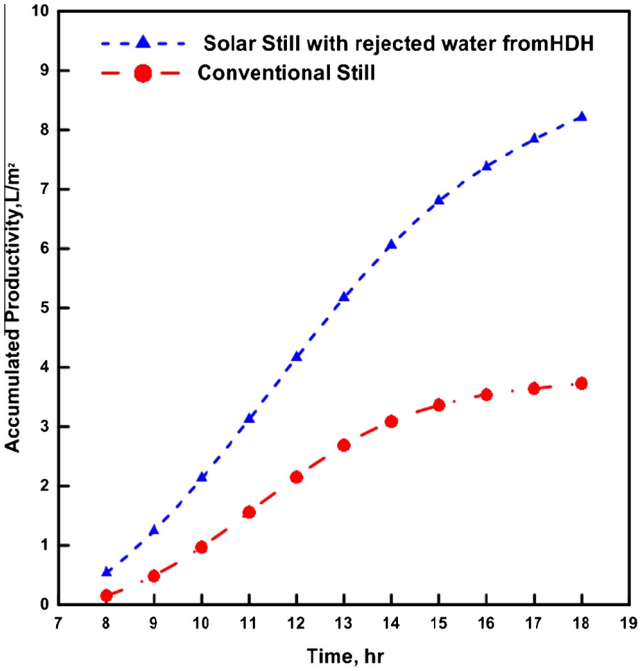


**Fig. 9.** Accumulative variation of freshwater for the SS with water rejected from HDH and the CSS during the daytime.

and CSS is illustrated in Fig. 8. From the figure, it is found that the average maximum freshwater productivity at noon has the highest values for the present solar desalination systems. In addition, the higher water production is observed in SS with water exit warm from HDH compared with CSS type. This is due to high temperature of water in the SS from insulation tank at all time and does not need time to warm up (change all water in the basin occurs every hour from storage tank at $T_w$ = 70 °C during 24 h), but temperature of water in the CSS is low in the early morning and water needs more time to warm up. In addition, the figure shows that a wide productivity change was recorded. Fig. 8 shows that the

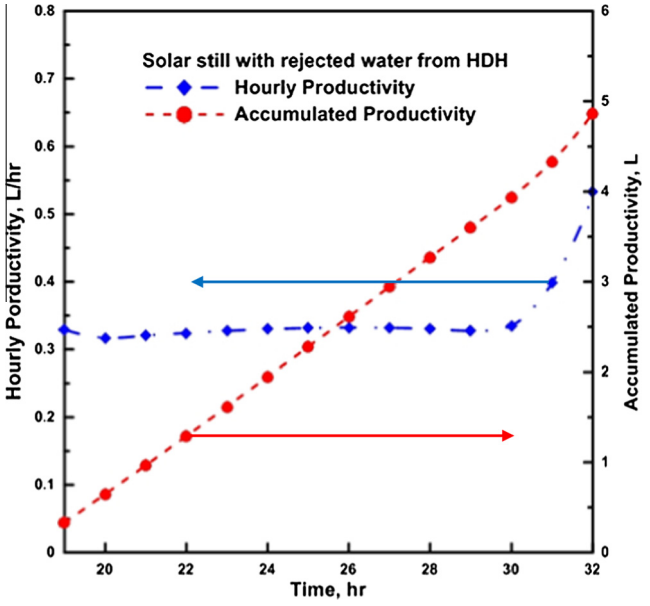


**Fig. 10.** Hourly and accumulated output during the nighttime from SS with rejected water from HDH.

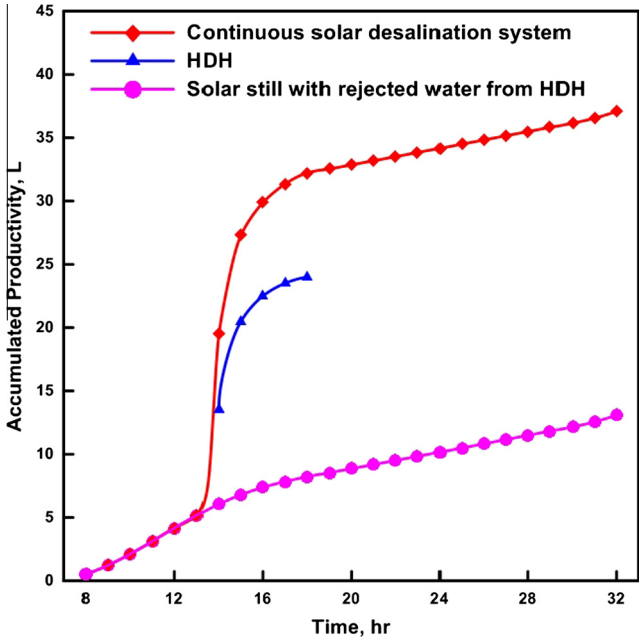


**Fig. 11.** Accumulated productivity during 24 h for SS, HDH and HDH–SS.

water productivity was around 0.58 and 0.07 L/m$^2$ h in the early mornings, reaching up to 1.15 and 0.6 mL/m$^2$ h as a maximum productivity at 12 pm for SS with exit warm water from HDH and CSS, respectively. Therefore, the performance has the best value at the mid-noon where the losses are minimal.

### 6.6. Water productivity during the daytime from solar stills

Fig. 9 shows a theoretical comparison between the average hourly accumulative variations of freshwater productivity from 9 am to sunset. It is found that the amount of accumulated distillate for SS with HDH is higher than that of CSS at all time, where the average hourly freshwater productivity is higher for SS with exit warm water from HDH. In addition, the distillate reaches 3.62 and 8.2 L/daytime for CSS and SS with exit warm water from HDH, respectively. In this case, the increase in distillate production for SS with water exit warm from HDH is 126.5% higher than that of CSS type.

### 6.7. Effect of feeding warm water during nighttime on the stills productivity

Fig. 10 illustrates the average prediction of the alteration of freshwater output per hour (from 19 pm to 8 am of the second day) of SS during night times at inlet water temperatures of about 70 °C. The ambient air temperature is in the range of 17–26 °C, whereas wind velocity is in the range of 1.2–4.5 m/s during the average measurement day. During the early hours of the night, the temperature difference between the SS and surroundings increases as the air temperature decreases, and hence, more heat losses happen. As a result, the productivity decreases. Furthermore, the first hours of the second day cause an increase in the productivity due to sunrise, decrease the temperature difference between the still and the surrounds and heat losses decrease. In addition, the distillate reaches 0.2 and 4.8 L/nighttime for CSS and SS with exit warm water from HDH, respectively.

**Table 4**
Comparison between present study and different research works about HDH or CSS systems.

| References | Productivity (L/day) |
|---|---|
| *Present study* | |
| Solar still with rejected water from HDH | 13 |
| HDH system | 24 |
| Continuous solar desalination system | 37 |
| Nafey et al. [5,6], HDH | 10.25 |
| Hamed et al. [7], HDH | 22 |
| Omara et al. [31], CSS | 2.7 |

### 6.8. Continuous system productivity

Fig. 11 shows the accumulative freshwater of the system during daytimes and nighttime's. The accumulative freshwater production improves with strengthening the solar radiation intensity and vice versa. The daily water production of the SS with exit warm water from HDH, HDH and continuous system (HDH + SS with rejected water from HDH) are 13, 24 and 37 L/day, respectively.

## 7. Comparison between present work with other research work

Comparison between present study and different research works about HDH or CSS systems are tabulated in Table 4.

## 8. Conclusions

Performances of a continuous solar desalination system consisting of HDH unit and SS have been studied. It was noticed that small HDH unit or SS unit individually is not efficient for desalination of brackish water and seawater. The best performance of HDH is obtained at feed water flow rate of 2.5 L/min. Reusing the exit warm water increases, the highest productivity of SS with exit warm from HDH by about 242%; and increases the GOR of the system by about 39%. The daily water production of the CSS, SS with rejected water from HDH, HDH system and continuous solar desalination system are 3.9, 13, 24 and 37 L/day, respectively.

## Acknowledgements

N.Y. was sponsored by the National Natural Science Foundation of China Grant (No. 51576076).

## Appendix A

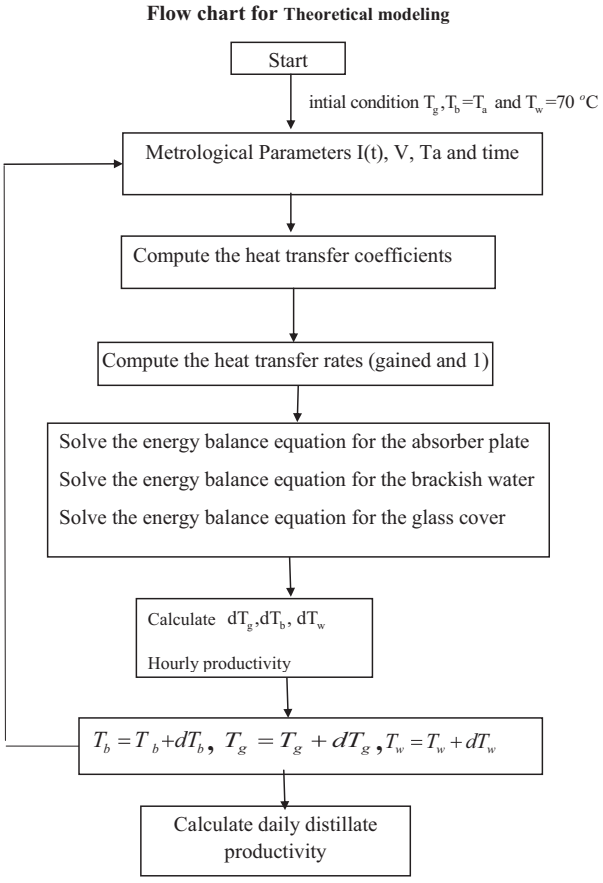


## References

[1] G. Venkatesan, S. Iniyan, P. Jalihal, A theoretical and experimental study of a small-scale barometric sealed flash evaporative desalination system using low grade thermal energy, Appl. Therm. Eng. 73 (2014) 629–640.
[2] M. Elimelech, The global challenge for adequate and safe water, J. Water Supply: Res. Technol. – Aqua 55 (2006) 3–10.
[3] G.P. Narayan, M.H. Sharqawy, E.K. Summers, J.H. Lienhard, S.M. Zubair, M.A. Antar, The potential of solar-driven humidification–dehumidification desalination for small-scale decentralized water production, Renew. Sustain. Energy Rev. 14 (2010) 1187–1201.
[4] A. Kabeel, M. Hamed, Z. Omara, S. Sharshir, Water desalination using a humidification–dehumidification technique—a detailed review, Nat. Resour. 4 (2013) 286–305.
[5] A.S. Nafey, H.E.S. Fath, S.O. El-Helaby, A.M. Soliman, Solar desalination using humidification dehumidification processes. Part I. A numerical investigation, Energy Convers. Manage. 45 (2004) 1243–1261.
[6] A.S. Nafey, H.E.S. Fath, S.O. El-Helaby, A. Soliman, Solar desalination using humidification–dehumidification processes. Part II. An experimental investigation, Energy Convers. Manage. 45 (2004) 1263–1277.
[7] M.H. Hamed, A.E. Kabeel, Z.M. Omara, S.W. Sharshir, Mathematical and experimental investigation of a solar humidification–dehumidification desalination unit, Desalination 358 (2015) 9–17.
[8] S. Hou, D. Zeng, S. Ye, H. Zhang, Exergy analysis of the solar multi-effect humidification–dehumidification desalination process, Desalination 203 (2007) 403–409.
[9] K. Zhani, Solar desalination based on multiple effect humidification process: thermal performance and experimental validation, Renew. Sustain. Energy Rev. 24 (2013) 406–417.
[10] C. Yıldırım, İ. Solmuş, A parametric study on a humidification–dehumidification (HDH) desalination unit powered by solar air and water heaters, Energy Convers. Manage. 86 (2014) 568–575.
[11] S. Hou, H. Zhang, A hybrid solar desalination process of the multi-effect humidification dehumidification and basin-type unit, Desalination 220 (2008) 552–557.
[12] Y.H. Zurigat, M.K. Abu-Arabi, Modelling and performance analysis of a regenerative solar desalination unit, Appl. Therm. Eng. 24 (2004) 1061–1072.
[13] A.K. Tiwari, G.N. Tiwari, Effect of water depths on heat and mass transfer in a passive solar still: in summer climatic condition, Desalination 195 (2006) 78–94.
[14] M. Abu-Arabi, Y. Zurigat, H. Al-Hinai, S. Al-Hiddabi, Modeling and performance analysis of a solar desalination unit with double-glass cover cooling, Desalination 143 (2002) 173–182.
[15] S.W. Sharshir, N. Yang, G. Peng, A.E. Kabeel, Factors affecting solar stills productivity and improvement techniques: a detailed review, Appl. Therm. Eng. 100 (2016) 267–284.
[16] K. Voropoulos, E. Mathioulakis, V. Belessiotis, Experimental investigation of the behavior of a solar still coupled with hot water storage tank, Desalination 156 (2003) 315–322.
[17] A.F. Muftah, M.A. Alghoul, A. Fudholi, M.M. Abdul-Majeed, K. Sopian, Factors affecting basin type solar still productivity: a detailed review, Renew. Sustain. Energy Rev. 32 (2014) 430–447.
[18] Y.P. Yadav, Analytical performance of a solar still integrated with a flat plate solar collector: thermosiphon mode, Energy Convers. Manage. 31 (1991) 255–263.
[19] R. Tripathi, G.N. Tiwari, Thermal modeling of passive and active solar stills for different depths of water by using the concept of solar fraction, Sol. Energy 80 (2006) 956–967.
[20] M.A. Eltawil, Z. Zhengming, Wind turbine-inclined still collector integration with solar still for brackish water desalination, Desalination 249 (2009) 490–497.
[21] N. Setoodeh, R. Rahimi, A. Ameri, Modeling and determination of heat transfer coefficient in a basin solar still using CFD, Desalination 268 (2011) 103–110.
[22] R. Tchinda, E. Kaptouom, D. Njomo, Heat and mass transfer processes in a solar still with an indirect evaporator–condenser, Energy Convers. Manage. 41 (2000) 93–107.
[23] A.E. Kabeel, M.H. Hamed, Z.M. Omara, S.W. Sharshir, Experimental study of a humidification–dehumidification solar technique by natural and forced air circulation, Energy 68 (2014) 218–228.
[24] J.-J. Hermosillo, C.A. Arancibia-Bulnes, C.A. Estrada, Water desalination by air humidification: mathematical model and experimental study, Sol. Energy 86 (2012) 1070–1076.
[25] V. Velmurugan, S. Pandiarajan, P. Guruparan, L.H. Subramanian, C.D. Prabaharan, K. Srithar, Integrated performance of stepped and single basin solar stills with mini solar pond, Desalination 249 (2009) 902–909.
[26] K. Kalidasa Murugavel, S. Sivakumar, J. Riaz Ahamed, K.K.S.K. Chockalingam, K. Srithar, Single basin double slope solar still with minimum basin depth and energy storing materials, Appl. Energy 87 (2010) 514–523.
[27] V. Velmurugan, S. Senthil Kumaran, V. Niranjan Prabhu, K. Srithar, Productivity enhancement of stepped solar still – performance analysis, Therm. Sci. 12 (2008) 153–163.
[28] V. Velmurugan, K.J. Naveen Kumar, T. Noorul Haq, K. Srithar, Performance analysis in stepped solar still for effluent desalination, Energy 34 (2009) 1179–1186.
[29] R. Dev, G.N. Tiwari, Characteristic equation of a passive solar still, Desalination 245 (2009) 246–265.
[30] V. Velmurugan, C.K. Deenadayalan, H. Vinod, K. Srithar, Desalination of effluent using fin type solar still, Energy 33 (2008) 1719–1727.
[31] Z.M. Omara, A.E. Kabeel, M.M. Younes, Enhancing the stepped solar still performance using internal reflectors, Desalination 314 (2013) 67–72.